horticulturae

MDPI

Article

The Effect of Host-Induced *Me-chs-1* Gene Silencing on the Pathogenicity of *Meloidogyne enterolobii*

Shanquan Duan, Jinying Gu, Xuelan Wang, Wentao Wu, Songmei Chen, Yuezhang Guan, Qian Gao and Yang Wang *

Key Laboratory of Agricultural Biodiversity and Pest Control, College of Plant Protection, Yunnan Agricultural University, Kunming 650201, China; 18387278445@163.com (S.D.); fungijinyinggu@163.com (J.G.); 15687478013@163.com (X.W.); wentao_wu121@163.com (W.W.); chensongmei99@163.com (S.C.); 17787362128@163.com (Y.G.); 15969443098@163.com (Q.G.)

* Correspondence: wangyang626@sina.com

Abstract

Meloidogyne enterolobii, is a devastating pathogen capable of overcoming conventional resistance genes. This study presents the first investigation into targeting the chitin synthase gene *Me-chs-1* in *M. enterolobii* using host-induced gene silencing (HIGS). Our results demonstrate that HIGS effectively suppresses *Me-chs-1* expression, leading to a drastic reduction in nematode reproductive capacity, with the most effective transgenic line showing over 82% decrease in total egg production. Additionally, notable developmental deformities were observed in the nematodes. This study confirms *Me-chs-1* as a promising target for controlling *M. enterolobii* and lays a solid foundation for developing novel resistance breeding strategies and eco-friendly nematicides.

Keywords: *M. enterolobii*; HIGS; RNAi; transcriptome sequencing technology

check for updates

Academic Editors: Carmelo Peter Bonsignore and Francesco Lops

Received: 19 June 2025
Revised: 26 September 2025
Accepted: 14 October 2025
Published: 20 October 2025

Citation: Duan, S.; Gu, J.; Wang, X.; Wu, W.; Chen, S.; Guan, Y.; Gao, Q.; Wang, Y. The Effect of Host-Induced *Me-chs-1* Gene Silencing on the Pathogenicity of *Meloidogyne enterolobii*. *Horticulturae* **2025**, *11*, 1265. https://doi.org/10.3390/horticulturae11101265

Copyright: © 2025 by the authors. Licensee MDPI, Basel, Switzerland. This article is an open access article distributed under the terms and conditions of the Creative Commons Attribution (CC BY) license (https://creativecommons.org/licenses/by/4.0/).

1. Introduction

Root-knot nematodes (*Meloidogyne* spp.) are sedentary endoparasitic nematodes that infect plant roots and have a broad geographic distribution [1]. They inflict severe economic damage, causing global annual losses estimated at up to USD 100 billion [2], and have emerged as major phytopathogens worldwide [3]. Upon penetrating the root cortex, these nematodes establish specialized feeding sites and secrete effector proteins—such as cellulases and pectinases—that induce abnormal cell division, leading to the formation of root galls or tumor-like structures of varying sizes [4]. Initially, these galls appear white or yellowish white; they later turn brown and decay, causing severe deformities in the root system that impede normal water and nutrient uptake. Although gall formation is often accompanied by an apparent increase in the number of lateral and fine roots, the functional root surface area is reduced, further compromising the plant's ability to absorb soil resources. These pathological changes ultimately manifest aboveground as stunted growth and leaf chlorosis, and in severe cases, lead to wilting and plant death [5,6]. For example, melon plants infected with root-knot nematodes become dwarfed and chlorotic, with poorly developed fruits [7], while the yields of tomato, cucumber, and other vegetables can decline by more than 50% due to root damage [8]. In addition to directly consuming plant nutrients, root-knot nematode infection damages root tissues, creating entry points for fungal, bacterial, and viral pathogens, and thereby precipitating secondary diseases such as root rot and wilt [9,10].

Over 100 species of root-knot nematodes (RKNs) have been described; the most prevalent include *Meloidogyne incognita*, *Meloidogyne hapla*, *Meloidogyne arenaria*, *Meloidogyne javanica*, and *Meloidogyne enterolobii* [11,12]. Among these, *M. enterolobii* (syn. *M. mayaguensis*) is considered one of the most virulent RKN species due to its ability to infect and reproduce in host plants that possess resistance against major tropical RKNs [13]. It was first reported in 1983 on pacara earpod tree (*Enterolobium contortisiliquum*) in Danzhou, Hainan Province, China [14]. Compared with closely related species such as *M. incognita* and *M. javanica*, *M. enterolobii* causes more severe damage. It alone can lead to yield losses of up to 65%, which is higher than those caused by any other root-knot nematode species studied to date [15]. Zhang et al. confirmed that the minimum infective dose of *M. enterolobii* on tomato is 0.08 J2 per cm^3 of soil, compared to 1.0 J2/cm^3 for *M. incognita* and 0.64 J2/cm^3 for *M. javanica*. Subsequent gall counts, egg mass counts, and reproduction indices were also significantly higher for *M. enterolobii* than for other species [16]. Its distribution is primarily tropical and subtropical but is expanding into higher latitude regions—a trend expected to accelerate under global warming and the increased use of protected agriculture with soil heating [17]. Moreover, *M. enterolobii* can overcome multiple plant resistance genes—such as the *Mi-1* gene in tomato, *Mh* in potato, *N* in pepper, *Tabasco* in sugar beet, and *Mir1* in soybean [18–21]—rendering conventional resistant cultivars ineffective, whereas these genes remain effective against other root-knot nematodes. Therefore, further research on *M. enterolobii* and the development of effective control strategies are critically important [22].

Chitin, a linear polymer of β-1,4–linked N-acetylglucosamine, is an abundant structural polysaccharide [23]. It is primarily found in the cell walls of fungi, the exoskeletons of arthropods (such as insects, crustaceans), and the eggshells and cuticles of nematodes [24,25]. In contrast, plants have cell walls composed mainly of cellulose, hemicellulose, and pectin, and they lack the metabolic pathways to synthesize chitin [26,27]. Since chitin is an essential component of nematode eggshells and cuticles, disruption of chitin synthesis or hydrolysis leads to embryonic lethality, defective egg-laying, or molting failure in nematodes. Thus, key components of the chitin metabolic pathway are promising targets for the development of anti-nematode agents [28]. The chitin biosynthesis pathway involves three key steps: substrate generation, chitin polymerization, and modification/deposition. First, glucose undergoes a series of metabolic reactions catalyzed by hexokinase, glucose-6-phosphate isomerase, and other related enzymes to produce UDP-*N*-acetylglucosamine (UDP-GlcNAc), the direct substrate for chitin synthesis. Subsequently, chitin synthase, localized on the cell membrane, catalyzes the linkage of *N*-acetylglucosamine units via β-1,4-glycosidic bonds to form linear, unbranched chitin polymers. Finally, the synthesized chitin chains undergo further modifications and are deposited in structures such as cell walls, insect exoskeletons, nematode eggshells, and other specialized compartments [24]. Notably, chitin synthase plays a pivotal role in this process, as its activity and regulation critically determine the quantity and quality of the chitin produced [29]. Previous studies have shown that silencing chitin synthase genes in plant-parasitic nematodes enhances host resistance [30,31]. Although *M. enterolobii* also has a triploid genome like its relatives, its unique symmetric differentiation of subgenomes results in greater gene redundancy and higher evolutionary adaptability [32]. Therefore, the effectiveness of silencing a single gene in *M. enterolobii*, such as the chitin synthase gene, remains to be verified. To date, no such study has been reported.

This study aimed to develop a novel control strategy based on host-induced gene silencing (HIGS) by targeting the chitin synthase gene (*Me-chs-1*) of *M. enterolobii*. The full-length sequence of this gene was cloned and subjected to bioinformatic analysis. HIGS was employed to knock down the expression of the chitin synthase gene in *M. enterolobii*, and its control efficacy was validated through inoculation with second-stage juveniles (J2).

This research provides important insights into the function and mechanism of the chitin synthase gene, while laying a foundation for breeding *M. enterolobii*-resistant crop varieties and developing novel environmentally friendly nematicides.

2. Materials and Methods

2.1. Plant and Nematode Materials

Tested tomato variety: The susceptible tomato cultivar Microtom, preserved by the Nematology Laboratory of Yunnan Agricultural University, Kunming, China.

Root-knot nematode source: *M. enterolobii* was collected, purified, and propagated by the Nematology Laboratory of Yunnan Agricultural University. Live nematodes were maintained in the root systems of the highly susceptible tomato cultivar Zhongshu No. 4 and water spinach (*Ipomoea aquatica*).

2.2. Total RNA Extraction

Tomato seedlings infected with *M. enterolobii* were rinsed with distilled water, and root galls containing eggs were collected as extraction samples. Total RNA was isolated using the TransZol Up Plus RNA Kit (TransGen Biotech Co., Ltd., Beijing, China). RNA concentration and purity were measured using a NanoDrop™ 2000 spectrophotometer (Thermo Fisher Scientific Inc., Walthem, MA, USA). RNA integrity was further verified via 1% agarose gel electrophoresis. High-quality RNA (A260/A280 = 1.8–2.0, clear ribosomal bands) was reverse-transcribed into cDNA using the PrimeScript™ RT Reagent Kit (Takara Bio Inc., Kusatsu, Shiga, Japan) with gDNA Eraser.

2.3. Cloning of the Full-Length CDS of the Chitin Synthase Gene

Using cDNA as the template, the cloning was performed in two segments, separately obtaining the 5′ and 3′ CDS fragments, which were then assembled into the pUC19 vector using the ClonExpress Ultra One Step Cloning Kit V2 (Vazyme Biotech Co., Ltd., Nanjing, Jiangsu, China) to generate the full-length CDS of the chitin synthase gene.

Primers (5′ end F/R, 3′ end F/R and Seamless cloning primers F/R) were designed using the online primer design software CE Design (https://tool.vazyme.com:18002/cetool/singlefragment.html, accessed on 12 August 2024).

2.4. Sequence Alignment and Functional Analysis

The cDNA sequences were aligned and analyzed using DNAMAN (Version 9), and their nucleotide sequences were translated into amino acid sequences. Conserved domains were identified via the CD-Search tool at the National Center for Biotechnology Information (NCBI) (http://www.ncbi.nlm.nih.gov/blast/, accessed on 24 September 2024). The amino acid sequences of chitin synthase were retrieved from the NCBI and WormBase (https://wormbase.org/ accessed on 25 September 2024) databases. Multiple sequence alignment and phylogenetic tree construction were conducted using MEGA (Version 11.0).

2.5. Construction of the Gene Silencing Vector and Agrobacterium-Mediated Transformation of Tomato

An RNAi construct targeting the conserved domain of the *Me-chs-1* gene was generated. Three primer pairs—tatF$^+$/tatF$^-$, loop$^+$/loop$^-$, and tatR$^+$/tatR$^-$—were designed against the target region. The tatF$^+$/tatF$^-$ and tatR$^+$/tatR$^-$ fragments were PCR-amplified from a plasmid harboring the *Me-chs-1* CDS, whereas the loop$^+$/loop$^-$ fragment was amplified from the pCTAG11-GUSPlus vector. (Primer sequences are provided in Appendix B). PCR products were resolved on a 1% agarose gel, and the bands corresponding to the expected sizes were excised and purified. Purified PCR fragments were then cloned into the pBWA(V)HS vector via homologous recombination to yield recombinant plasmids

under the control of the CaMV 35S promoter. Following transformation into *Escherichia coli*, positive clones were identified using colony PCR and confirmed via Sanger sequencing; plasmids from verified clones were further validated by using EcoRV restriction analysis. The confirmed RNAi constructs were introduced into *Agrobacterium tumefaciens* strain GV3101 via heat shock. Transformants containing the target insert were selected and stored at –80 °C. Finally, tomato cotyledons were transformed using the *Agrobacterium*-mediated transformation system. T_0 transgenic plants were screened by PCR to confirm genomic integration of the RNAi cassette, and T_1 seeds were harvested for downstream experiments.

2.6. Inoculation of T_1 Generation Seedlings with M. enterolobii and Pathological Analysis

Seeds of T_1 transgenic and wild-type tomato lines were surface-sterilized by immersion in 6% sodium hypochlorite for 7 min, followed by thorough rinsing with sterile water. The seeds were germinated on moist filter paper at 25 °C until radicle emergence and then transferred to seedling trays for further growth. When the seedlings developed 4–5 true leaves, they were transplanted into the trays and placed in a solar greenhouse maintained at 25 °C under a 10-h light/14-h dark photoperiod. Four holes, approximately 1–2 cm in depth, were made around the base of each seedling using a 1 mL pipette tip at a distance of about 1 cm from the stem. A suspension containing 500 J2 juveniles of *M. enterolobii* was inoculated evenly into the root zone through these holes.

Root samples from three biological replicates were collected at 2, 8, 16, 23, and 30 days post-inoculation (dpi) and stained using the sodium hypochlorite–acid fuchsin–glycerol method as described by Byrd et al. [33],to observe nematode infection and developmental stages. At 45 dpi, the following parameters were recorded for both wild-type and RNAi transgenic lines: number of egg masses, number of galls, number of eggs per mass, and total egg count. Individual galls were excised and treated with 6% sodium hypochlorite for 4–5 min to dissolve the gelatinous matrix; released eggs were counted under a stereomicroscope. The total egg count was extrapolated based on triplicate counts of 100 µL aliquots taken from the nematode egg suspension. The gall formation percentage was calculated and classified according to the grading standards established by Yan et al. [34].

2.7. qRT-PCR Analysis of Chitin Synthase Gene Expression

At 45 dpi, three biological replicates were collected from both T_1 transgenic tomato plants and wild-type controls. Total RNA of nematodes was extracted following the protocol described in Section 2.2 and reverse-transcribed into cDNA. The *Actin* gene of *M. enterolobii* was used as the internal reference, with amplification primers Me-Actin-F/Me-Actin-R, gene-specific qPCR primers Me-QP-F/Me-QP-R were designed based on the CDS of the chitin synthase gene. qRT-PCR was performed to quantify the relative expression of the target gene.

2.8. Effect of Silencing the Chitin Synthase Gene on the M. enterolobii Transcriptome

At 45 dpi with *M. enterolobii*, root samples were collected from three biological replicates each of the RNAi line (ZT3) and the wild-type control. Then twenty female adults were manually picked out from the root knots of each root system. Total RNA of nematodes was extracted according to the protocol described in Section 2.2, and subsequently reverse-transcribed into cDNA. RNA sample concentration and purity were assessed spectrophotometrically, and those samples meeting the quality criteria for high-throughput sequencing were submitted to Shanghai Paiseno Biotechnology Co., Ltd. for transcriptome sequencing. Subsequently, the sequencing reads were compared to the reference genome of the *M. enterolobii* (accession number: PRJEB69523) using TopHat2 software (Version 2.1.0), and quantitative gene expression analysis was performed by Cufflinks software (Ver-

sion 2.2.4) to screen out differentially expressed genes. Then the GO and KEGG enrichment analysis were conducted.

2.9. Statistical Analysis

All experiments in this study included at least three independent biological replicates. Unless otherwise specified, each sample was assayed with three technical replicates. Data are presented as the mean ± standard deviation (Mean ± SD). Parameters related to nematode infection (such as the number of root knots, egg masses, etc.) and gene expression data were visualized using bar graphs, where the bar height represents the mean and the error bars represent the standard deviation.

To evaluate the differences in infection parameters and gene expression levels between wild-type and RNAi transgenic lines, Student's *t*-test was used for comparisons between two groups. For comparisons involving more than two groups, one-way analysis of variance (One-way ANOVA) was employed, followed by appropriate post hoc tests (such as Tukey's HSD test) for multiple comparisons. In all statistical analyses, a *p*-value less than 0.05 ($p < 0.05$) was considered statistically significant.

3. Result

3.1. Cloning and Bioinformatics Analysis of the Chitin Synthase Gene

Four putative chitin synthase genes in *M. enterolobii* were identified through NCBI database searches: CAD2169478.1, CAD2180532.1, CAK5089395.1, and CAK5088075.1. Sequence alignment revealed that these genes ranged in length from 3684 to 3840 bp (Figure 1). With high sequence homology (97.69%) among the four genes, primers targeting conserved regions were designed to clone the chitin synthase genes from *M. enterolobii*.

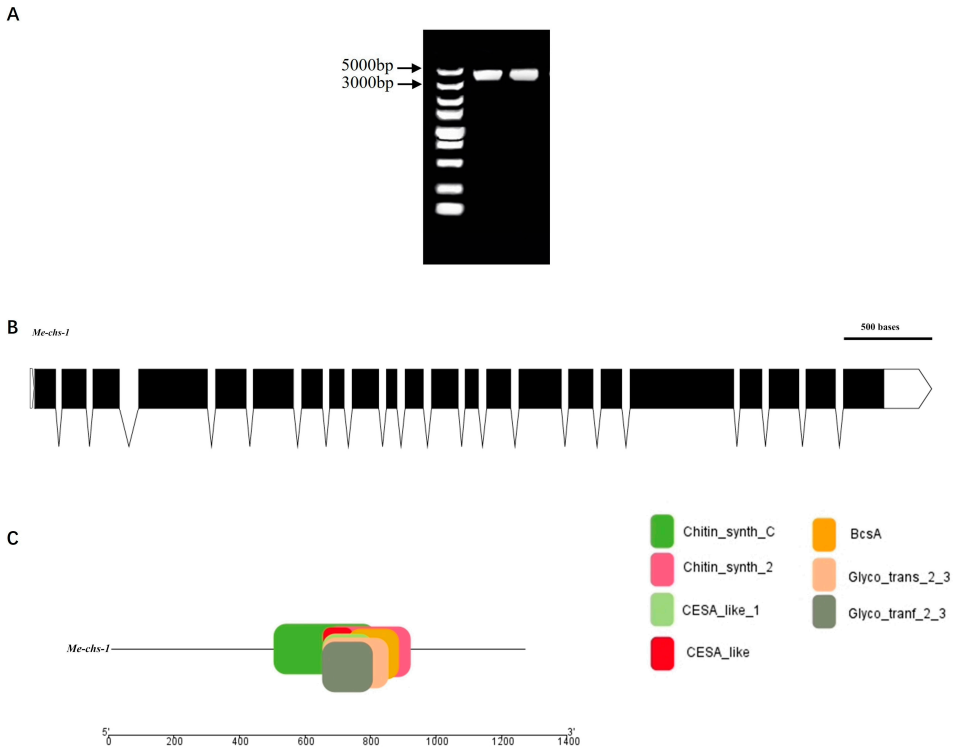


Figure 1. Full-length sequence and gene structure of chitin synthase gene. (**A**) Electropherogram of the full-length CDS sequence of chitin synthase gene. (**B**) Nucleotide structure diagram: white trapezoids represent untranslated regions (UTRs), black quadrilaterals indicate exon regions, and the regions between the black line segments correspond to intron regions. (**C**) Conserved domain structure diagram.

The gene was successfully cloned, with a coding sequence (CDS) length of 3788 bp (Figure 1A). It contains 22 exons and 21 introns, encoding a protein composed of 1261 amino acids. Conserved domain analysis identified seven conserved domains in the gene: Chitin Synthase C, Chitin Synthase 2, CESA-like, CESA-like 1, BcsA, Glyco_trans_2_3, and Gly-co_trans_2_3 (Figure 1C). Notably, Chitin Synthase C and Chitin Synthase 2 are catalytic domains characteristic of chitin synthase genes, confirming the successful cloning of chitin synthase genes from *M. enterolobii*.

A phylogenetic tree was constructed for the proteins encoded by chitin synthase genes from different species. Phylogenetic assessment (Figure 2) showed that among the four chitin synthase genes of *M. enterolobii*, the cloned gene exhibited the highest amino acid sequence homology with the chitin synthase of *M. incognita* (Wormbase database accession number: Minc3s00218g07846). In addition, the chitin synthase genes of *M. enterolobii* had a relatively close evolutionary relationship with the *chs-1* gene of *C. elegans* (GenBank accession number: G5ECD6.1), while the homology with the *chs-2* gene of *C. elegans* (GenBank accession number: G5EBQ8.1) was significantly lower. Based on this conserved evolutionary pattern and functional orthology, the cloned chitin synthase gene of *M. enterolobii* was systematically designated as *Me-chs-1*.

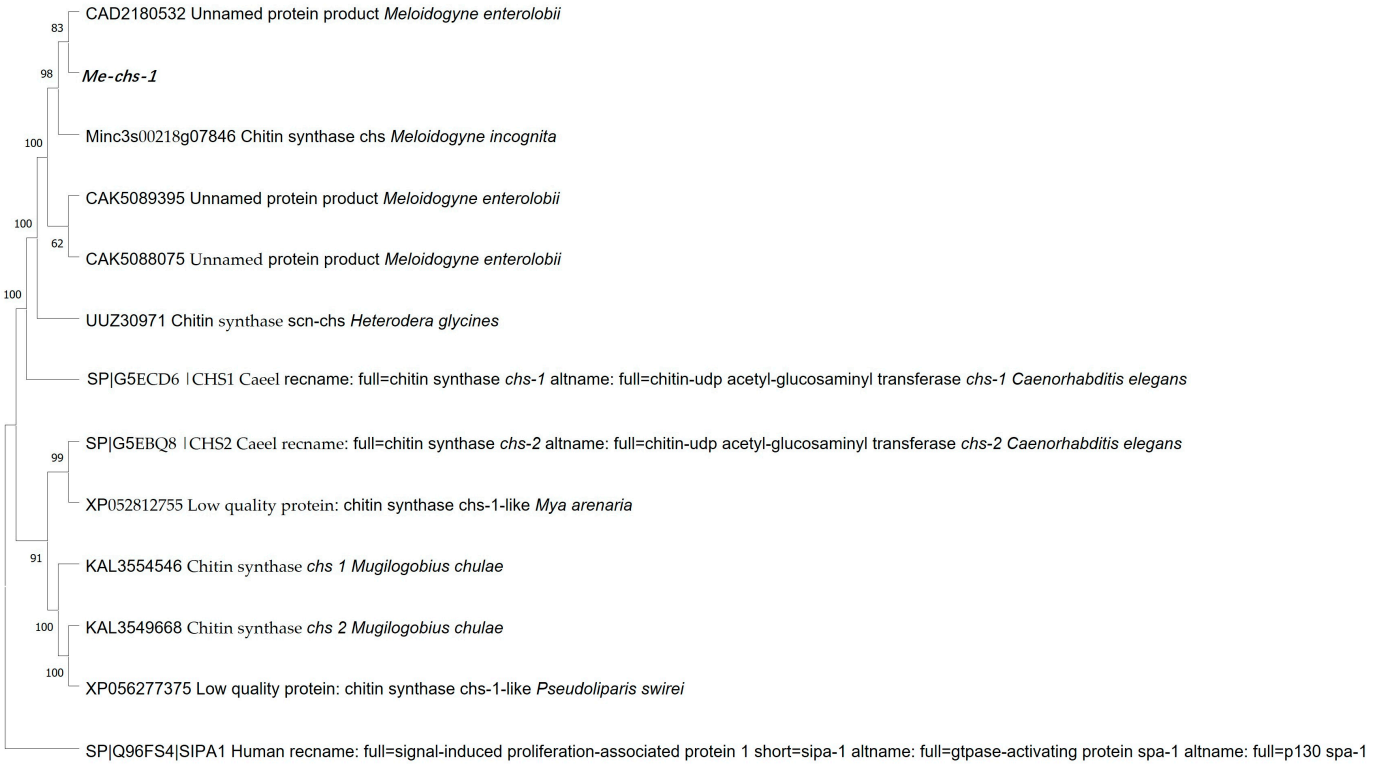


Figure 2. Phylogenetic tree of *Me-chs-1* and homologous proteins based on amino acid sequence. The evolutionary tree was constructed using the Neighbor-Joining method in MEGA 11. The optimal tree is shown. The percentage of replicate trees in which the associated taxa clustered together in the bootstrap test (1000 replicates) are shown next to the branches. The evolutionary distances were computed using the p-distance method and are in the units of the number of amino acid differences per site.

3.2. Construction of Gene Silencing Vectors

Three RNAi silencing vectors—pBWA(V)HS-Chitin Synthase Gene Silencing 1-RNAi (ZT1), pBWA(V)HS-Chitin Synthase Gene Silencing 2-RNAi (ZT2), and pBWA(V)HS-Chitin Synthase Gene Silencing 3-RNAi (ZT3)—were successfully constructed (Figure 3). These vectors target three distinct conserved domains of the chitin synthase gene: 1497–1698 bp

(5′ end of the Chitin synthase_C domain), 1736–1950 bp (3′ end of the Chitin synthase_C domain), and 2207–2408 bp (spanning regions homologous to Chitin Synthase 2, CESA-like, CESA-like 1, BcsA, Glyco_trans_2_3, and Glyco_trans_2_3 domains).

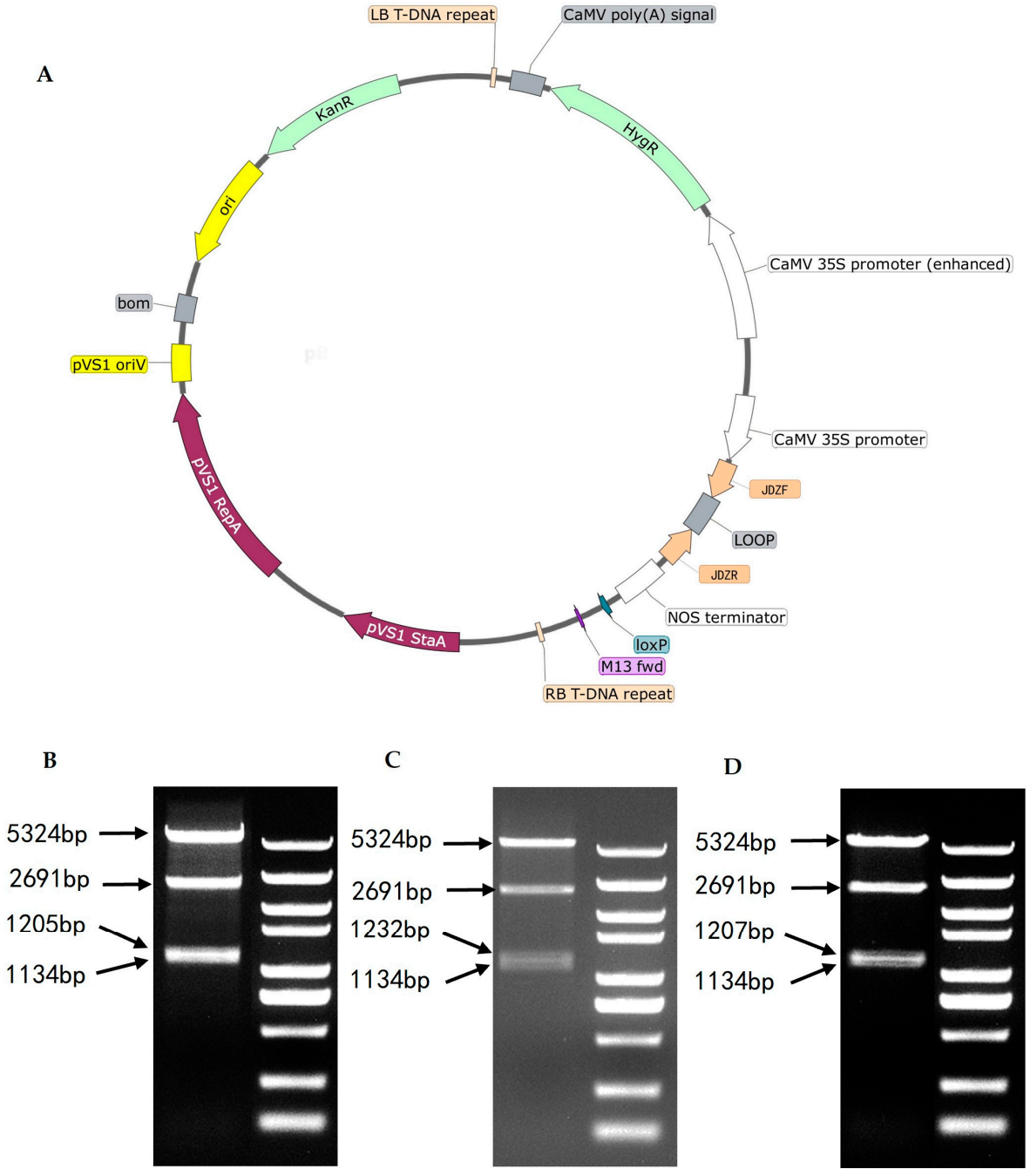


Figure 3. Schematic diagram of the silencing vector structure and restriction enzyme digestion identification results. (**A**) Schematic diagram of the RNAi silencing vector construct. "JDZF" indicates forward fragment of target region; "JDZR"indicates reverse fragment of target region. (**B**–**D**) EcoRV restriction enzyme digestion verification of ZT1, ZT2, and ZT3. The constructed silencing vector contains four EcoRV restriction sites. Digestion with EcoRV generates four fragments: 5324 bp, 2691 bp, 1134 bp, and 1205–1232 bp. Electrophoresis results should theoretically display 3–4 bands (the two fragments around 1000 bp may not be resolved as distinct bands). The three bands observed in the ZT1, ZT2, and ZT3 lanes confirm successful vector construction.

3.3. The Expression Levels of Chitin Synthase Genes After Gene Silencing

The relative expression levels of the *Me-chs-1* gene in wild-type plants (CK) and RNAi lines (ZT1, ZT2, and ZT3) were analyzed via qRT-PCR at 45 days post-inoculation with *M. enterolobii* (Figure 4A). The results revealed that all three RNAi vectors efficiently silenced the gene compared to CK, with expression levels in ZT1, ZT2, and ZT3 reduced to 25.75%, 14.9%, and 6.87% of those in CK, respectively. Silencing efficiency varied among the vectors, with ZT3 exhibiting the strongest suppression of *Me-chs-1*. Furthermore, transcriptome sequencing results for the ZT3 strain targeting *M. enterolobii* revealed reduced expression levels of four putative chitin synthase genes (CAD2169478.1, CAD2180532.1, CAK5089395.1, and CAK5088075.1) compared to the wild type (Figure 4B).

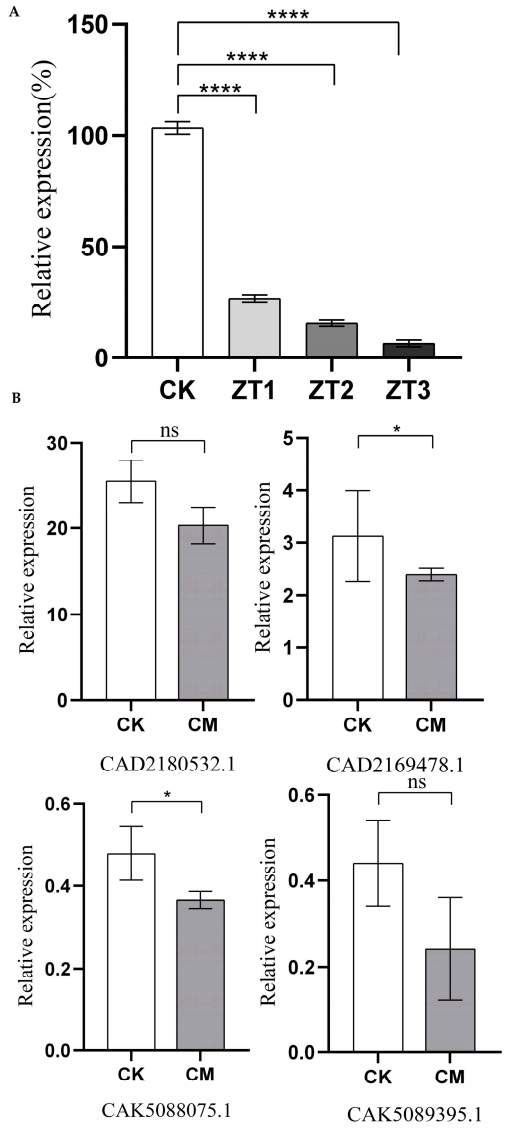


Figure 4. The expression levels of chitin synthase genes after gene silencing CK represents the wild-type tomato; (**A**) Expression levels of chitin synthase genes in wild-type and gene-silenced lines (ZT1, ZT2, and ZT3).(**B**) Expression levels of the four chitin synthase genes in wild-type and ZT3 lines. CM denotes the gene-silenced tomato; ZT1-ZT3 represent T1-generation tomato lines harboring gene-silencing vectors, respectively. AS shown by ANOVA, and error bars represent standard error of three biological and three technical replicates (n = 9), "ns" indicates non-significant differences, "*" denotes significant differences ($p < 0.05$), and "****" represents extremely significant differences ($p < 0.0001$).

Notably, the fold-reduction in CAK5089395.1 and CAK5088075.1 exceeded that observed for CAD2169478.1 and CAD2180532.1. Among the four genes, CAD2180532.1 displayed the highest baseline expression, suggesting that CAD2180532.1 may serve as the predominant chitin synthase gene in *M. enterolobii* under the current experimental conditions.

3.4. Impact of Me-chs-1 Silencing on Cumulative Infection Rate and Developmental Progression in M. enterolobii

Analysis of cumulative infection rates at 2, 8, 16, 23, and 30 dpi revealed no significant differences between RNAi lines (ZT1-ZT3) and wild-type (CK) controls during the early infection stages (2–16 dpi) (Figure 5). However, on days 23 and 30, the cumulative penetration rates in the RNAi lines were lower than those in CK, suggesting that silencing of the *Me-chs-1* gene may impair the nematode's later-stage development and penetration ability, thereby reducing the cumulative invasion rate.

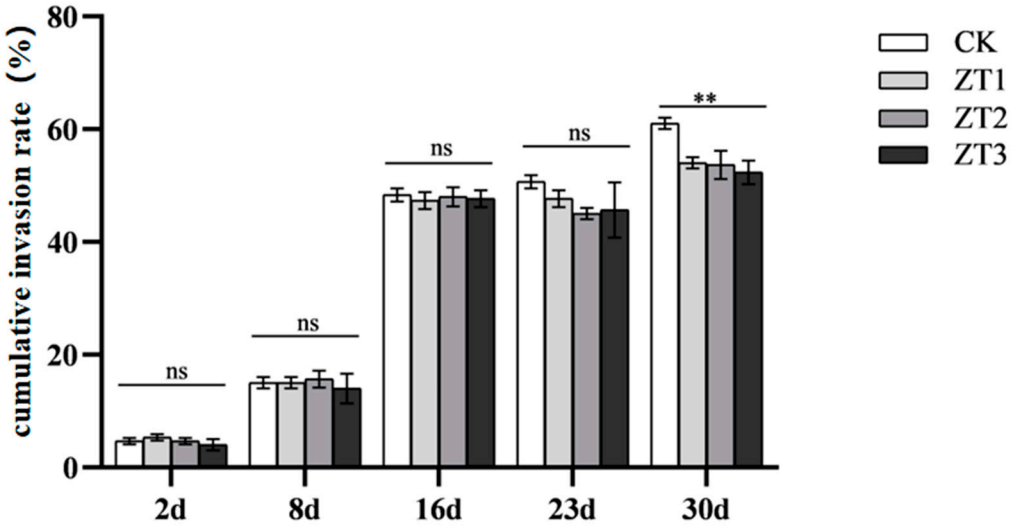


Figure 5. Time-course accumulation of *M. enterolobii* infections in *Me-chs-1* RNAi and wild-type (CK) tomato strains; ZT1-ZT3 represent T1-generation tomato lines harboring gene-silencing vectors, respectively. The horizontal lines in the figure indicate the significance analysis of CK with ZT1, ZT2 and ZT3 respectively. AS shown by ANOVA, and error bars represent standard error of three biological replicates (n = 3), "ns" indicates non-significant differences, "**" denotes significant differences ($p < 0.05$).

We also evaluated nematode developmental stages in CK and the three RNAi lines (ZT1, ZT2, and ZT3) at the same five time points (Figure 6). In CK roots, nematode development proceeded normally: by day 16 they had reached the third juvenile stage, by day 23 they exhibited initial female morphology, and by day 30 they were fully developed females. In contrast, although nematode development in ZT1, ZT2, and ZT3 did not differ significantly from CK from day 2 to day 16, between days 23 and 30 development was markedly delayed in all three RNAi lines, with juveniles remaining smaller than those in the wild type. Notably, in ZT3-treated roots, nematodes were not only smaller at days 2 and 30 but also displayed developmental deformities. These results indicate that RNAi-mediated silencing of *Me-chs-1* suppresses middle- and late-stage development of *M. enterolobii*, with the strongest effect observed in ZT3.

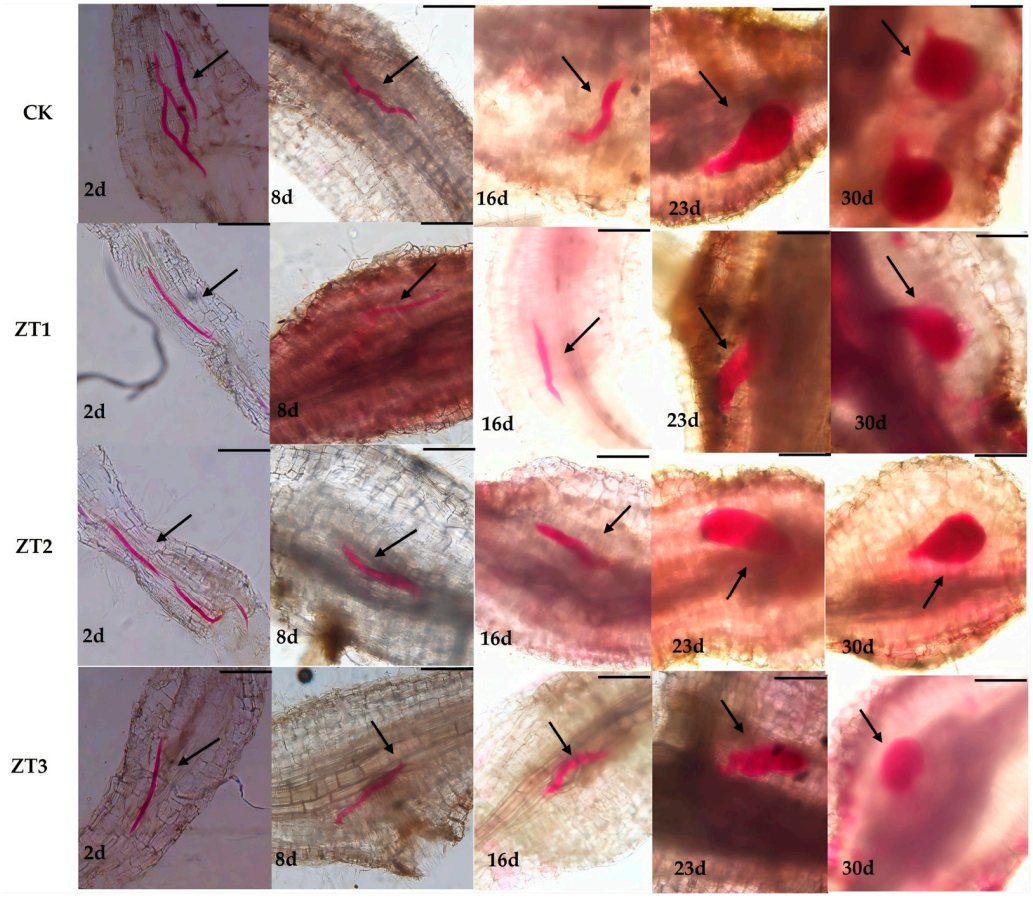


Figure 6. Development in the roots after inoculation with *M. enterolobii* in RNAi and wild-type (CK) tomato strains. ZT1–ZT3 represent T1-generation tomato lines harboring gene-silencing vectors, respectively. Black arrows indicate nematode morphology, red areas represent stained root-knot nematodes, and the remaining regions show tomato root tissue. The developmental stages of the nematodes at different time points are clearly observable.

3.5. Effects of Me-chs-1 Gene Silencing on the Pathogenicity of M. enterolobii

We compared root symptoms between RNAi tomato lines and the wild-type tomato line (CK) following inoculation with *M. enterolobii* (Figure 7). The RNAi lines had significantly fewer root galls and smaller gall diameters than CK did, indicating that silencing *Me-chs-1* impairs nematode establishment and feeding site development.

In addition, we quantified several pathological parameters—root galling percentage, root galling index, gall number, egg mass number, eggs per mass, and total egg count—for CK and the three RNAi lines (ZT1, ZT2, and ZT3) (Table 1). CK showed a gall incidence of 46.02%, whereas ZT1, ZT2, and ZT3 had values of 35.13%, 34.77%, and 30.72%, representing reductions of approximately 23.7%, 24.5%, and 33.2%, respectively. This demonstrates that *Me-chs-1* silencing lowers the root-knot nematode infection rate.

The average gall count in CK was 67± 7.41, compared with 32 ± 36 (ZT1), 19 ± 4.55 (ZT2), and 16 ± 7.26 (ZT3)—reductions of about 52.2%, 71.6%, and 76.1%, respectively—confirming a significant decrease in gall formation due to RNAi treatment.

Egg mass counts also dropped markedly: CK produced 17 ± 5.31 masses, while ZT1, ZT2, and ZT3 yielded 11 ± 4.19, 8 ± 4.99, and 3 ± 1.25, respectively, respectively, representing reductions of 35.3%, 52.9%, and 82.4% compared to the CK group. Correspondingly, eggs per mass decreased from 402 ± 18.98 in CK to 236 ± 36.5 (ZT1), 209 ± 42.21 (ZT2), and 151 ± 36.55 (ZT3), respectively, with decreases of 41.3%, 48.0%, and 62.4%. Total egg counts fell from 5940 ± 146.97 in CK to 1260 ± 146.97 (ZT1), 1320 ± 224.5 (ZT2),

and 1027 ± 224.5 (ZT3), respectively, with decreases as high as 78.8%, 77.8%, and 82.7%. These results clearly indicate that *Me-chs-1* silencing substantially reduces the reproductive capacity of *M. enterolobii*.

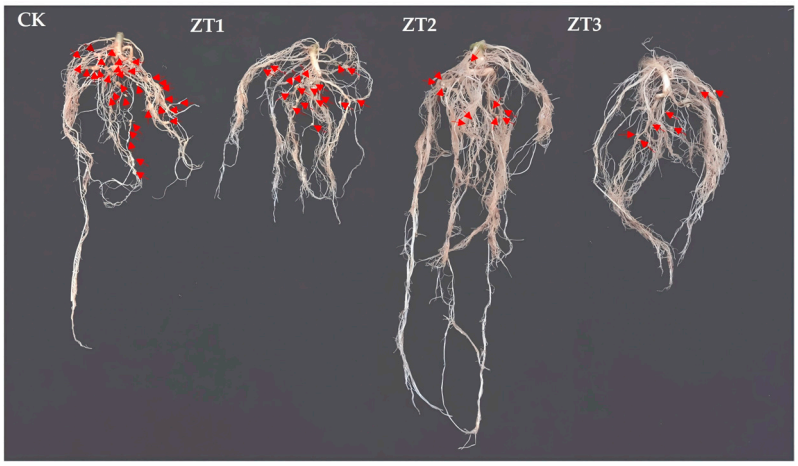


Figure 7. Root symptom phenotypes of RNAi tomato strains and wild-type tomato strains (CK) at 45 days post-inoculation with *M enterolobii*. ZT1–ZT3 represent T1-generation tomato lines harboring gene-silencing vectors, respectively. The red arrows point to the root galls; the more arrows there are, the greater the number of root galls.

Table 1. Pathological evaluation of RNAi tomato strains and wild-type tomato strains (CK) at 45 days post-inoculation with *M enterolobii*.

	Root Galling Percentage	Root Galling Index	Gall Number	Egg Mass Number	Eggs per Mass	Total Egg Count
CK	46.02%	3	67 ± 7.41 a	17 ± 5.31 a	402 ± 18.98 a	5940 ± 136.8 a
ZT1	35.13%	3	32 ± 7.36 b	11 ± 4.19 ab	236 ± 36.5 b	1260 ± 146.9 b
ZT2	34.77%	3	19 ± 4.55 b	8 ± 4.99 ab	209 ± 42.21 bc	1320 ± 213.4 b
ZT3	30.72%	3	16 ± 7.26 b	3 ± 1.25 b	151 ± 36.55 c	1027 ± 224.5 b

ZT1–ZT3 represent T1-generation tomato lines harboring gene-silencing vectors, respectively. Data were analyzed by ANOVA with Duncan's multiple test. Different lowercase letters indicate statistically significant differences ($p < 0.05$).

3.6. Differential Gene Expression and Functional Annotation

The pathological staining results indicated that chitin synthase gene silencing predominantly impairs the late-stage growth and development of *M. enterolobii*; accordingly, samples at 45 days post-inoculation (45 dpi) were selected for transcriptome sequencing. Comparative transcriptome analysis of nematodes in ZT3 RNAi tomato lines (CM) and in wild-type tomato lines (CK) at 45 days post-inoculation (45 dpi) with *M. enterolobii* revealed 501 differentially expressed genes (DEGs) (Figure 8A), of which 230 were upregulated and 271 downregulated in CM relative to CK. Gene Ontology (GO) analysis was performed on the 501 DEGs, yielding annotations for 350 genes. These DEGs were classified into the three main GO categories: molecular function (MF), cellular component (CC), and biological process (BP) (Figure 8B). In the MF category, the most enriched terms were "structural constituent of cuticle," "structural molecule activity," and "L-glutamate transmembrane transporter activity," with genes associated with cuticle structure markedly more abundant than those for other terms. Under CC, the largest clusters were "eRF1 methyltransferase complex," "excitatory synapse," and "acetylcholine-gated channel complex." For BP, the DEGs were primarily associated with "membrane repolarization during action potential" and general "membrane repolarization." KEGG pathway enrichment analysis revealed that 128 DEGs were significantly enriched (Figure 8C). The top enriched pathways included

the Wnt signaling pathway, spliceosome, ferroptosis, and ABC transporters, with the Wnt signaling pathway exhibiting the highest number of associated DEGs.

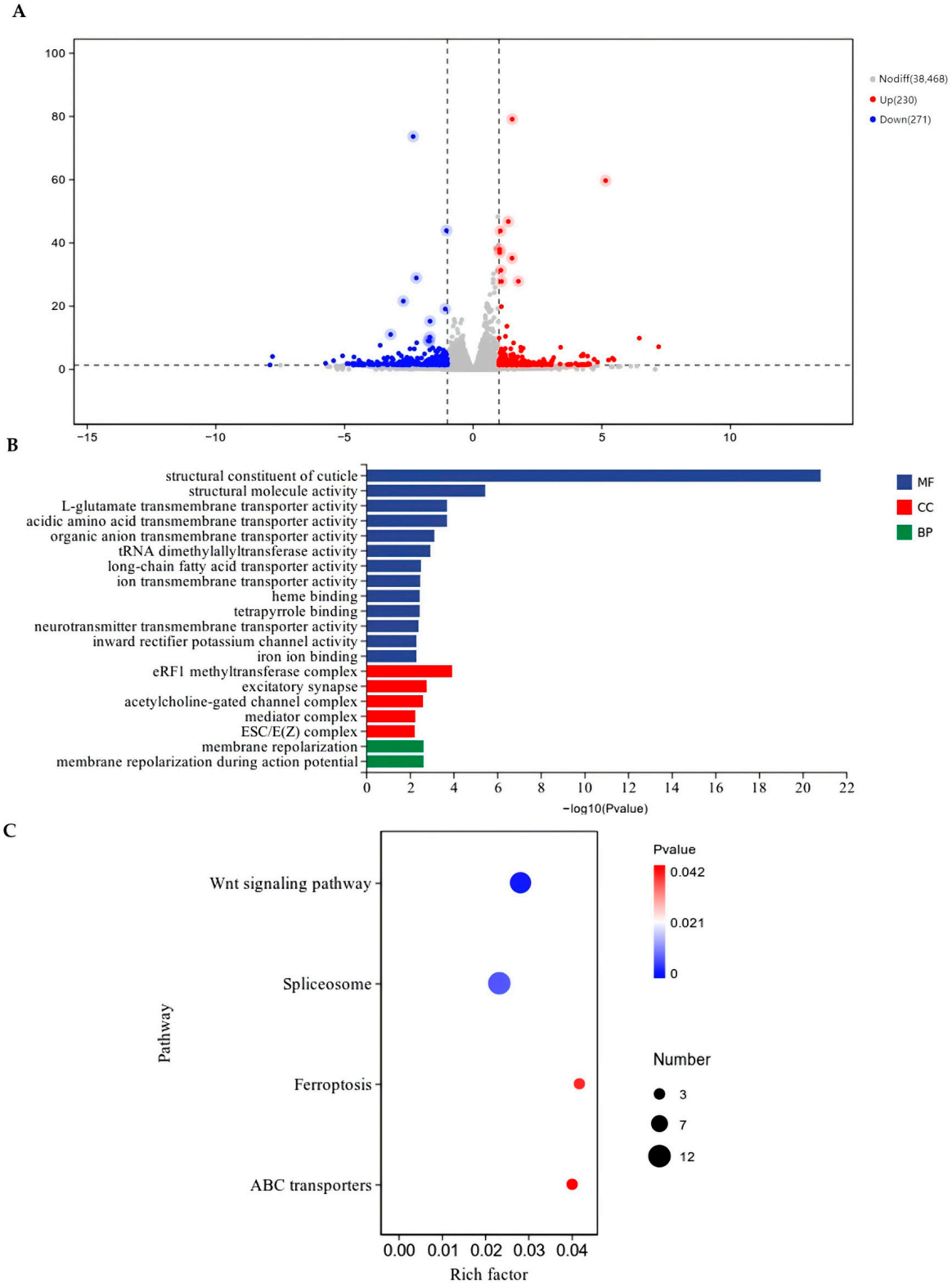


Figure 8. Transcriptome analysis of *M enterolobii* in RNAi transgenic lines and wild-type plants (ZT3 vs. CK) at 45 dpi. (**A**) Volcano plot of differential gene expression. (**B**) GO functional annotation of differential genes. (**C**) Bubble plot of KEGG enrichment analysis for differentially expressed genes. The color of the point represents *p*-value, and the size of the point represents the number of differentially enriched metabolites.

4. Discussion

In 1996, Baulcombe first discovered that double-stranded siRNA could silence genetic material in nematodes [35].Two years later, Fire and Mello further reported the RNAi phenomenon and revealed the molecular mechanism of double-stranded RNA (dsRNA)-mediated gene silencing [36]. These two studies laid the theoretical foundation for the application of RNAi technology. In 2002, Urwin and colleagues achieved in vitro RNAi silencing of target genes in infective larvae of *Globodera pallida* and *Heterodera glycines* for the first time by mediating oral uptake of dsRNA molecules with a neurostimulant [37], opening the door to the application of this technology in research and control of plant-parasitic nematodes. Studies on the model nematode *C. elegans* have shown that RNAi technology can protect crops by targeting essential nematode genes [38]. Based on this, researchers proposed two core strategies: targeting plant genes involved in the infection process or directly targeting essential nematode genes. The idea of accumulating hpRNA (hairpin RNA) containing key nematode gene sequences in host plants and delivering dsRNA to nematodes via feeding to inactivate their genes has made RNAi the preferred method in plant nematology research due to its high efficiency in inhibiting nematode growth, which has been confirmed effective in gene silencing of root-knot nematodes (*Meloidogyne* spp.) and cyst nematodes [39].Target genes for nematode gene silencing need to meet conditions such as parasitic survival necessity, functional specificity, and RNAi sensitivity, including cell wall degrading enzyme genes, molting and development regulatory genes, etc. *CHS* genes, as key genes in the chitin synthesis pathway, are selected as RNAi targets for controlling root-knot nematode diseases. This is because chitin is an important component of nematode eggshells, and chitin is absent in plants, so this strategy not only meets the criteria for gene silencing targets but also has the advantages of high efficiency and safety.

To validate the control potential of chitin synthase genes against nematodes, we used Host-Induced Gene Silencing (HIGS) technology to target the essential gene *Me-chs-1* of *Meloidogyne enterolobii*. Results showed that after silencing *Me-chs-1*, the number of root knots, egg masses, eggs per egg mass, and total eggs in tomato lines were significantly reduced, consistent with findings in *Meloidogyne incognita* and *Heterodera glycines*: Mani et al. reduced root knots and egg masses by over 60% and altered female nematode morphology via silencing the chitin synthase gene of *M. incognita* [30]; Kong et al. observed an 83.3% reduction in cyst numbers and 37.5% reduction in eggs per cyst after silencing this gene in *H. glycines* [31]. Notably, this study further revealed that gene silencing decreased nematode invasion rate and caused late-stage developmental disorders: Acid fuchsin staining showed significantly fewer invading nematodes in RNAi-treated roots at 23 and 30 days post-inoculation, with smaller, developmentally delayed larvae and obvious malformations in the ZT3 line. This indicates that *Me-chs-1* not only affects nematode reproduction but also regulates late developmental stages (e.g., molting or cuticle formation), supplementing earlier research with distinct findings.

To explore the mechanism of chitin synthase gene silencing, we performed transcriptome sequencing on the ZT3 line with the strongest silencing effect and wild-type nematodes, finding significant down regulation of four chitin synthase genes in *M. enterolobii* and identifying 501 differentially expressed genes (DEGs), of which most of 271 downregulated genes were significantly enriched in "chitin structural component"-related functions by GO analysis. Notably, KEGG annotation showed that DEGs were primarily enriched in the Wnt signaling pathway—a conserved cellular signaling network involved in nematode embryonic development, cell differentiation, and molting [40,41]. Although no study has directly confirmed the association between the Wnt pathway and chitin metabolism, com-

bining our data, we propose that members of the Wnt pathway can also serve as potential targets for the management of *M. enterolobii*.

Given the remarkable ability of *M. enterolobii* to overcome multiple resistance genes and the current scarcity of effective resistance resources, our experimental results demonstrate that chitin synthase gene silencing enhances tomato resistance to *M. enterolobii* infection. Considering the absence of chitin synthesis pathways in plants and mammals, thus ensuring minimal impact on non-target organisms, *CHS* genes emerge as highly promising targets for combating plant pests through. Disrupting *CHS* activity through genetic, chemical, or biological interventions has shown promising results in reducing nematode infestations. RNAi has enabled a pivotal breakthrough in nematode control through targeted silencing of *CHS* genes, effectively disrupting chitin synthesis. Key advantages of RNAi include its species-specificity and minimal environmental impact. However, challenges persist, including the effective delivery of dsRNA to nematodes and the risk of off-target effects. Our research revealed that the strategy targeting chitin synthase alone exhibit limited effectiveness on reducing *M. enterolobii* infestations, underscoring the necessity for enhanced RNA interference efficiency. Targeting 2–3 unique, pest-specific genes simultaneously (e.g., chitin synthase + a unique digestive enzyme) reduces dependence on a single sequence, thereby minimizing safety risks from off-target effects. Additionally, microbial agents producing chitinolytic enzymes (e.g., *Streptomyces* spp.) degrade nematode eggshells, indirectly affecting CHS activity [42]. Therefore, future work should prioritize integrating synergistic approaches (e.g., combining RNAi with microbial degradation) alongside developing nematode-resistant crops through gene editing. Additionally, chitin biosynthetic pathway-targeting pesticides offer high efficacy and environmental benefits [43], commercial chitin-targeting agrochemicals—like nikkomycins against fungi [44] and benzoylurea insecticides [45]—remain undeveloped for nematode control. Integrating these chemical approaches with the previously discussed RNAi and microbial biocontrol agents within an integrated pest management (IPM) framework offers the most sustainable and resilient strategy for managing *M. enterolobii* and related pests, potentially reducing reliance on broad-spectrum chemicals with greater environmental footprints [22].

5. Conclusions

M. enterolobii possesses four candidate chitin synthase genes CAD2169478.1, CAD2180532.1, CAK5089395.1, and CAK5088075.1, exhibiting an overall sequence homology of 97.69%. The coding sequence (CDS) of the *Me-chs-1* gene spans 3788 base pairs, encoding a protein of 1261 amino acids. This protein shows the highest homology to the chitin synthase protein of *M. incognita*. Furthermore, the proteins encoded by all four chitin synthase genes display high homology with the *chs-1* protein of *C. elegans*.

Silencing the chitin synthase gene in *M. enterolobii* effectively reduces its invasion, suppresses its growth and development, and inhibits its reproduction; thereby, tomato resistance to root-knot nematodes was enhanced. Transcriptomic analysis of differentially expressed genes indicates a potential indirect regulatory relationship between the Wnt signaling pathway and chitin metabolism.

This study represents the first systematic validation of the efficacy of HIGS technology targeting the *Me-chs-1* gene against *M. enterolobii*, which not only expands the understanding of chitin synthesis biological functions but also provides a novel target for nematode-resistant crop breeding. Follow-up research should further conduct field efficacy trials and explore multi-target synergistic silencing strategies with other critical genes (such as parasitism essential genes or effector genes) to promote the transition of RNAi technology from laboratory research to field application.

Author Contributions: Conceptualization, S.D. and Y.W.; methodology, S.D., J.G., X.W. and Q.G.; software, W.W.; validation, S.C., Y.G. and Q.G.; formal analysis, W.W.; investigation, S.D. and J.G.; resources, S.D. and J.G.; data curation, Y.W. and W.W.; writing—original draft preparation, S.D.; writing—review and editing, S.D. and Y.W.; visualization, S.D. and J.G.; supervision, Y.W.; project administration, Y.W.; funding acquisition, Y.W. All authors have read and agreed to the published version of the manuscript.

Funding: This work was supported by national natural science foundation of China project (32160618).

Data Availability Statement: The original contributions presented in the study are included in the article, further inquiries can be directed to the corresponding author.

Conflicts of Interest: The authors declare no conflicts of interest.

Appendix A. Full-Length Coding Sequence (CDS) of the Me-chs-1 Gene and Three Target Sequences for Silencing Vectors

ATGCTTTTTTACCGCGATCACCACCAGTGGGATGCATTTAGGACTCACCCTCGA
ATTAAACGTACACCGCAAAAATCTCACGCTTATTACATTCGTTGGTTACAATGGTTAA
AGTTGATCATTTTTGTAATTTCCCATTGTTCTTCACTTGTGGCTGTGCTCGTTTCCAAA
TCTGTAATTATCCTTCTCTCAACTAACATTGGACTTAACTATATTATGGCTGACACAAA
ATTCTATGGACATTGCAAAAGCCCCTCAACTGACCAAGATTTTGACCGATTGAGTTC
AATTTGTGCCGCTCTATGGCTTATTCAAACGATTCCAGATGTCTGCGCCTTTGTACAG
GATTTATTCAAAATTAGACTTACAACAAAAGCTGATCGTTCATTAATAGGAATGTTTA
TTCTTCTCGAATCTTTTCGAGCTACCGGACTTTCACTCGCCGTTTTGAATATATTTCCT
TTATTGGACGTTTCACGTTGTATAATGTTCACCTGTGCCTTTCACTGTTTCTACTACAT
CAAAAATGCCCTCCAAAATTTTCACCGTTCTTTTGACTTGAACCGTTCAATCCGCTG
GCGTTTTGCTTGCATTACCGCAAGTCTACCATCAGCTTTTCTTTTTGCCTTTCTATTTA
GTGCTGGCTATTTATGGGCACTTTTTGATGGTCATCCAAAGTTTAAATTTGGTGTGTTA
CTTACCATTTCTTTTACTCTATGTTCTCTTGGTTTTTGGGAGAGTTGGGTTGACACTAA
ACAAAAGGAGGGTCTTTTTCAAGAACTTTATGAGATTAAATATGGCATGAGAAAAC
TTAATCCAGAAACAAGAATGGTTGCTTCATTCCTTCGTTTTTTGTGCACGTCTTCAGT
TCTTTATTTTTCATTAAGGCATCATAATATTCCTGTTGGAACCTTAATTTTAATGCTATT
CAAAAGCAAAGAAGGAGTATTTGGAGATCAAGCAAAGATTTTCATATTTGCTTTTAT
TTCATTGGCACTCAATTTCTACCTTCGTATTTGCTTTCGTTTTTTGGCTGCAATGCGTC
TAAATTTGTTTACTTGTATCCATCCAGTGTTTTTATCAACTCCATTACTTTTAATGAGTT
TTCACGGATTATGTCATGTACTTCCAATTTGTCGGATCAACGTTATCTTAAAATATTTT
GATCTTAATTTGTTTTGTATCAAAGGTGTTAATCCTACTGGATCTGTAAAGGATTACTA
TATAACGTGGATTTGGTTATTTTCTTATATTATTTGGAGTTTAAAATTTACAAATGGGA
AGAAATATGACAAAACTGATGAAATAATTGAGTCGATGACACCAATGATGAGTGGA
TTGGATATTTGCCAGTCACTTGTTGTTTTTCGTTATTCAATTGCAAAGAAGGATGTTG
ACTACGACTCTGATGAAGATGTTGAGCCTGAGGAAAGCCCTCTTCGAATTATAAATG
GTCATATGGACAGAATTATTACTTTATATGTTTGTGCAACAATGTGGCATGAAACAA
AAAATGAAATGACGCAGATGCTTCGATCTATTCTAAAACTTGATGTTGAACAGTCT
GTCCGACAAAGCGAGGATGGAATCAAATTTCGATTAGAAATTCATATTTTCTTTGA
CGATGCTTGGGTTGATGACAGAGAATGTGGAAGAGTACCCAATGATTACTTCAAA
TTATTGTTTGATGTTTTAATTG(ZT1 target sequence)AGTTGACTAGATCAGAAAATGC
TGAAACAGACTTGTTTACACGTGTTCTTGTCAATACTCCTTATGGTGGACGTATTGT
TATGGCATTGAGTGGAGGCGCTCTTCTCTTTGTTCATCTTAAAGATAAGCGTTTAAT
TCGACATAAAAAGCGGTGGTCACAGGTTATGTATATGTACTATTTGCTTGGACACC
GAATTGTTGATTCTCATCTTAGCGTTGAAGATCGTCAATTACAAGCTGACAATACT
TACA(ZT2 target sequence)TTCTAGCAATTGATGGTGATTCAAAGTTTGAACCTTGTG
CTGTTCTTCGTTTGATTAACCTTATGAATCTAAAAAGTGATGTTGGTTGTGCCTGTGG
ACGTAATCATCCTATTGGAACTGGCGTAATGGTTTGGTATCAAAAGTTTGAATATGCA

ATTGCTCATTGGTTTCAAAAAGCAGCTGAACACGTCTTTGGATGTGTTTTATGCGCG
CCAGGTTGTTTCTCACTTTTTAGAGCATCAGCATTAATGGACGACAATATTATGAATA
AATACACAAAAACTGCTTCTGAACCAAGACATTTTGTCCAATATGACCAAGGTGA
AGATCGATGGCTTTCAACATTAATGCTTAAACAGGGTTATCGAATTGAATACGCTG
CTACTTCTGATGCAGAAACTTATGCACCTGAAGGTTTTGATGAATTCTTTAATCAA
AGGCGAAGGTGGACGCCATCT(ZT3 target sequence)TCAATTGCTAATACTTTGGAC
TTGTTGGCGGATTATAAGTTAGCTTCAAAAAACAATGCAAGCATTTCAAGGCTTTAT
ATTATATATCAAATGATTGTTATTGCATTTTCATTGCTTGGTCCTGCTATAATATTTACA
ATGCTTGTTTATGCTCAGGTTGCCGCTTTTGCTGTCGATTCAACGCGTGTTCTTGTTT
ACAATGCTATTCCAGTATGTGCATTTATTTGTTGTTGTTTTGCTTTGGATTCAAGCATTC
AATTGATATTTGCTAAAATTGCTTCTGTCGTTTATGCTTTCATAATGTTGGCTGTTCTC
ATCGCTACCACCAATCAAATTGTACTAGAAACAGTATTTTCACCAACATCAATGTTT
GTCCTTGGAATGGTTATTATTTTCTCATTTGCTTCATGCATTCATCCAAAAGAATTTTC
AAATATTATATTTGGAGCAATTTTCTTTTTGATGATTCCTTCAACTTATGTTTTTCTTTC
TCTTTATTCTTTAATCAATTTAAATGTGATCAATTGGGGTACAAGAGAAGCTGTTGCC
AAAGCTACTGGACAAACAACTTATAAAGAAAATATTGCAGAAAGAGTTCTGAGAA
GAGTTGCAAATTTAAACGATGAAAATTCTTTCCTTACAAGATTACTTATTCGATATCG
CGGTTCAGAAGAATCAAGCGCTAGGATACGAACTTTGGAAAGGAAAATTGAACGA
ACTGAACGTTTATTGCTTACAATAAAGGACTCAAATACATCAGTGGAATGTACACCA
GACAATAGAAGGTTTGGACGTCCGATGGATATGGTTGATGTAGTACTCAGAGAGGT
AAATGAGCCAGAATTGCCCATAAGGAGTGGTTATGAGGCTGTTGCCGTTCAACGGT
TACAAACTTTGCAGCGACATTCTGTTATTTCCGATCCTTGCAAACGTTCCCTTTGGAT
GGATTGTGAATATCTTCAATGTTGCGATCGAGGGAAGTTGCGTGCTGGTGAGGAAA
CATTTTGGGACGAACTTATTGACAGATATTTAAAGCCGATAGCATCAACCGCCCAAG
ATCAAGCTCAAATTGCTGCTGGTTTAGTTTCTTTGAGGAACAGAATTGCCTTCTCGAT
CATTTTGATGAATGGTTTGCTTGTCTTGGCTGTCTTTTTGCTTCAACGTCATAAAGATG
TTTTATCTGTAAAATTCATACTATACGAGGGCTTCAAATGGACAAAAATGAATGAAA
CAACAGGAAAATTTGAAGATACTACCGAAGCGCTAAAAGTTGATCCGCTTGGAATT
GGAATAATTTTCTTTTTGATGGGAATTCTTATAGTACAAACAATTGGGATGTTGATTC
ATCGCCTTAATACGTTAGTGGAAGCATTGCATGA

Appendix B. Primers

Vector	Primers	Primer Sequence (5′-3′)
5′ end	F	ATGCTTTTTTACCGCGATCACCAC
	R	CCTGTGACCACCGCTTTTTAT
3′ end	F	GTG-GAGGCGCTCTTCTCTTT
	R	CCAATCCATGACGTGTGTAACC
seamless cloning primers	F	aaaacgacggccagtgaattcATGCTTTTTTCCGCGATCACC
	R	gaccatgattacgccaagcttTCATGCAATGCTTCCACTAACG
Actin	F	AGTGCGACATTGACATCCGT
	R	TCGATGGTGCCAAAGCAGTA
Me-QP	F	ATGTGTTTTATGCGCGCCAG
	R	TCCGCCAACAAGTCCAAAGT

ZT1	tatF+	CAACTGGCATGAAACAAAAAATGAAATGACGC
	tatF-	CAGGCAATTAAAACATCAAACAATAATTTGAAGTAATCATTGGGT
	tatR+	GGGCCAATTAAAACATCAAACAATAATTTGAAGTAATCATTGGGT
	tatR-	CAACTGGCATGAAACAAAAAATGAAATGACGC
ZT2	tatF+	CAACACACGTGTTCTTGTCAATACTCCTTA
	tatF-	CAGGTGTAAGTATTGTCAGCTTGTAATTGACGATC
	tatR+	GGGCTGTAAGTATTGTCAGCTTGTAATTGACGATC
	tatR-	TACAACACGTGTTCTTGTCAATACTCCTTA
ZT3	tatF+	CAACACAATATTATGAATAAATACACAAAAACTGCTTC
	tatF-	GGGCAGATGGCGTCCACCTTCG
	tatR+	GGGCAGATGGCGTCCACCTTCG
	tatR-	TACAACAATATTATGAATAAATACACAAAAACTGCTTC
LOOP	loop+	CCTGCAGGTCTAGTTTTTCTC
	loop-	GCCCGGGCTCTGTAACTAT

References

1. Karssen, G. *The Plant Parasitic Nematode Genus Meloidogyne Göldi, 1892 (Tylenchida) In Europe*; Brill: Leiden, The Netherland, 2002.
2. Lianghong, C. Distribution and Identification of Root-Knot Nematodes in China. *Mod. Agric. Sci. Technol.* **2024**, *6*, 58–61.
3. Chang, L. Biological ControI of Vegetable Root—Knot Nematode. *Anhui Agri. Sci.* **2009**, *15*, 137–139.
4. Goverse, A.; Smant, G. The activation and suppression of plant innate immunity by parasitic nematodes. *Annu. Rev. Phytopathol.* **2014**, *52*, 243–265. [CrossRef]
5. Junhai, N.; Yangdong, G.; Heng, J. Progress in the Study of RNAi Mediated Plant Root-knot Nematodes Resistant Genetic Engineering. *Genom. Appl. Biol.* **2009**, *28*, 167–173.
6. Rugang, C. *Cloning and Identification of Root-Knot Nematode Resistance Genes in Tomato and Peppe*; Huazhong Agricultural University: Wuhan, China, 2006.
7. Xindi, W.; Yanqiu, C.; Lei, C.; Sen, Y.; Zeyu, S.; Chunfeng, S.; Changzheng, T. Research on the Control of Muskmelon Root-knot Nematodes by Returning Garlic Straw to the Field. *China Fruit Veg.* **2024**, *44*, 67–70+82. [CrossRef]
8. Daofeng, D.; Lifang, H.; Xiuhui, W. Rotation of resistant tomato and susceptible cucumber for control of root_knot nematode disease in greenhouses. *Plant Prot.* **2007**, *33*, 51–53.
9. Handoo, Z.; Skantar, A.; Carta, L.; Erbe, E. Morphological and molecular characterization of a new root-knot nematode, *Meloidogyne thailandica* n. sp.(Nematoda: Meloidogynidae), parasitizing ginger (*Zingiber* sp.). *J. Nematol.* **2005**, *37*, 343.
10. Qing, W.; Song, L.; Fengcheng, S.; Ruhong, Z. A Preliminary Study on Reduced Resistibility of Tobacco Plants to Black Shank Fungus Caused by Root Knot Nematodes. *Acta Agric. Boreali-Sin.* **1988**, *3*, 76–80.
11. Yujin, H.; Min, F.; Wenxiu, G.; Yi, Y. Overview of Integrated Control Techniques of Root-Knot Nematode Disease. *Shandong Acad. Agric. Sci.* **2019**, *51*, 149–156.
12. Jones, J.T.; Haegeman, A.; Danchin, E.G.; Gaur, H.S.; Helder, J.; Jones, M.G.; Kikuchi, T.; Manzanilla-López, R.; Palomares-Rius, J.E.; Wesemael, W.M. Top 10 plant-parasitic nematodes in molecular plant pathology. *Mol. Plant Pathol.* **2013**, *14*, 946–961. [CrossRef]
13. Chen, Y.; Liu, Q.; Sun, X.; Liu, L.; Zhao, J.; Yang, S.; Wang, X.; Quentin, M.; Abad, P.; Favery, B.; et al. *Meloidogyne enterolobii* MeMSP1 effector targets the glutathione-S-transferase phi GSTF family in *Arabidopsis* to manipulate host metabolism and promote nematode parasitism. *New Phytol.* **2023**, *240*, 2468–2483. [CrossRef] [PubMed]
14. Yang, B.; Eisenback, J. Meloidogyne enterolobii n. sp.(Meloidogynidae), a root-knot nematode parasitizing pacara earpod tree in China. *J. Nematol.* **1983**, *15*, 381. [PubMed]
15. Castagnone-Sereno, P. *Meloidogyne enterolobii* (=*M. mayaguensis*): Profile of an emerging, highly pathogenic, root-knot nematode species. *Nematology* **2012**, *14*, 133–138. [CrossRef]
16. Zhang, H.; Zhao, Z.; Chen, M. The effects of Meloidogyne enterolobii on the growth of seven tomato varieties. *Hainan Acad. Agric. Sci.* **2015**, *36*, 87–90.
17. Song, P.; Peng, D.-L.; Li, Y.-M.; Chen, Z.-J.; Zhai, Y.-Y.; Chen, L.; Bo, H. Potential global distribution of the guava root-knot nematode Meloidogyne enterolobii under different climate change scenarios using MaxEnt ecological niche modeling. *J. Integr. Agric.* **2023**, *22*, 2138–2150.
18. Brito, J.; Stanley, J.; Kaur, R.; Cetintas, R.; Di Vito, M.; Thies, J.; Dickson, D. Effects of the Mi-1, N and Tabasco genes on infection and reproduction of *Meloidogyne mayaguensis* on tomato and pepper genotypes. *J. Nematol.* **2007**, *39*, 327. [PubMed]

19. Kiewnick, S.; Dessimoz, M.; Franck, L. Effects of the Mi-1 and the N root-knot nematode-resistance gene on infection and reproduction of *Meloidogyne enterolobii* on tomato and pepper cultivars. *J. Nematol.* **2009**, *41*, 134.
20. Ye, W.; Koenning, S.; Zhuo, K.; Liao, J. First report of *Meloidogyne enterolobii* on cotton and soybean in North Carolina, United States. *Plant Dis.* **2013**, *97*, 1262. [CrossRef]
21. Berthou, F.; Kouassi, A.; Bossis, M.; Dantec, J.-P.; Eddaoudi, M.; Ferji, Z.; Pellé, R.; Taghzouti, M.; Ellissèche, D.; Mugniéry, D. Enhancing the resistance of the potato to southern root-knot nematodes by using Solanum sparsipilum germplasm. *Euphytica* **2003**, *132*, 57–65. [CrossRef]
22. Philbrick, A.N.; Adhikari, T.B.; Louws, F.J.; Gorny, A.M. *Meloidogyne enterolobii*, a Major Threat to Tomato Production: Current Status and Future Prospects for Its Management. *Front Plant Sci.* **2020**, *11*, 606395. [CrossRef]
23. Zhang, Y.; Foster, J.M.; Nelson, L.S.; Ma, D.; Carlow, C.K. The chitin synthase genes chs-1 and chs-2 are essential for *C. elegans* development and responsible for chitin deposition in the eggshell and pharynx, respectively. *Dev. Biol.* **2005**, *285*, 330–339. [CrossRef] [PubMed]
24. Yu, A.; Beck, M.; Merzendorfer, H.; Yang, Q. Advances in understanding insect chitin biosynthesis. *Insect Biochem. Mol. Biol.* **2024**, *164*, 104058. [CrossRef]
25. Kong, L.A.; Yang, J.; Li, G.T.; Qi, L.L.; Zhang, Y.J.; Wang, C.F.; Zhao, W.S.; Xu, J.R.; Peng, Y.L. Different chitin synthase genes are required for various developmental and plant infection processes in the rice blast fungus *Magnaporthe oryzae*. *PLoS Pathog.* **2012**, *8*, e1002526. [CrossRef]
26. Pusztahelyi, T. Chitin and chitin-related compounds in plant–fungal interactions. *Mycology* **2018**, *9*, 189–201. [CrossRef]
27. Sánchez-Vallet, A.; Mesters, J.R.; Thomma, B.P. The battle for chitin recognition in plant-microbe interactions. *FEMS Microbiol Rev.* **2015**, *39*, 171–183. [CrossRef]
28. Li, J.; Todd, T.C.; Lee, J.; Trick, H.N. Biotechnological application of functional genomics towards plant-parasitic nematode control. *Plant Biotechnol. J.* **2011**, *9*, 936–944. [CrossRef]
29. Tang, B.; Wei, P.; Zhao, L.; Shi, Z.; Shen, Q.; Yang, M.; Xie, G.; Wang, S. Knockdown of five trehalase genes using RNA interference regulates the gene expression of the chitin biosynthesis pathway in *Tribolium castaneum*. *BMC Biotechnol.* **2016**, *16*, 1–14. [CrossRef] [PubMed]
30. Mani, V.; Reddy, C.S.; Lee, S.-K.; Park, S.; Ko, H.-R.; Kim, D.-G.; Hahn, B.-S. Chitin biosynthesis inhibition of *Meloidogyne incognita* by RNAi-mediated gene silencing increases resistance to transgenic tobacco plants. *Int. J. Mol. Sci.* **2020**, *21*, 6626. [CrossRef] [PubMed]
31. Kong, L.; Shi, X.; Chen, D.; Yang, N.; Yin, C.; Yang, J.; Wang, G.; Huang, W.; Peng, H.; Peng, D. Host-induced silencing of a nematode chitin synthase gene enhances resistance of soybeans to both pathogenic *Heterodera glycines and Fusarium oxysporum*. *Plant Biotechnol. J.* **2022**, *20*, 809. [CrossRef]
32. Poullet, M.; Konigopal, H.; Rancurel, C.; Sallaberry, M.; Lopez-Roques, C.; Mota, A.P.Z.; Lledo, J.; Kiewnick, S.; Danchin, E.G. High-fidelity annotated triploid genome of the quarantine root-knot nematode, *Meloidogyne enterolobii*. *Sci Data* **2025**, *12*, 184. [CrossRef]
33. Bybd, D.W., Jr.; Kirkpatrick, T.; Barker, K. An improved technique for clearing and staining plant tissues for detection of nematodes. *J. Nematol.* **1983**, *15*, 142.
34. Yan, X.; Gao, Z.; Dong, Y.; Wu, W.; Zeng, Y.; Duan, S.; Wang, Y. Preliminary functional analysis of T106 gene specifically induced by *Meloidogyne enterolobii* in root-knot in tomato plants. *Acta Phytopathol. Sin.* **2024**, *54*, 950–960.
35. Baulcombe, D.C. RNA as a target and an initiator of post-transcriptional gene silencing in trangenic plants. *Plant Mol. Biol.* **1996**, *32*, 79–88. [CrossRef]
36. Fire, A.; Xu, S.; Montgomery, M.K.; Kostas, S.A.; Driver, S.E.; Mello, C.C. Potent and specific genetic interference by double-stranded RNA in *Caenorhabditis elegans*. *Nature* **1998**, *391*, 806–811. [CrossRef]
37. Dutta, T.K.; Banakar, P.; Rao, U. The status of RNAi-based transgenic research in plant nematology. *Front. Microbiol.* **2015**, *5*, 760. [CrossRef]
38. Bharathi, J.K.; Anandan, R.; Benjamin, L.K.; Muneer, S.; Prakash, M.A.S. Recent trends and advances of RNA interference (RNAi) to improve agricultural crops and enhance their resilience to biotic and abiotic stresses. *Plant Physiol. Biochem.* **2023**, *194*, 600–618. [CrossRef] [PubMed]
39. Mann, S.K.; Kashyap, P.L.; Sanghera, G.S.; Singh, G.; Singh, S. RNA interference: An eco-friendly tool for plant disease management. *Transgenic Plant J.* **2008**, *2*, 110–126.
40. Lie, D.-C.; Colamarino, S.A.; Song, H.-J.; Désiré, L.; Mira, H.; Consiglio, A.; Lein, E.S.; Jessberger, S.; Lansford, H.; Dearie, A.R. Wnt signalling regulates adult hippocampal neurogenesis. *Nature* **2005**, *437*, 1370–1375. [CrossRef]
41. Nusse, R.; Varmus, H.E. Wnt genes. *Cell* **1992**, *69*, 1073–1087. [CrossRef]
42. Atif, A.M.; Elzamik, F.I.; Mohamed, G.M.; Al-Quwaie, D.A.; Ashkan, M.F.; Alqahtani, F.S.; Motwali, E.A.; Alomran, M.M.; Alharbi, N.K.; El-Tarabily, K.A.; et al. Biological control of the root-knot nematode (*Meloidogyne incognita*) on eggplants with various chitinase-producing *Streptomyces* strains. *Eur. J. Plant Pathol.* **2023**, *167*, 371–394. [CrossRef]

43. Chen, W.; Cao, P.; Liu, Y.; Yu, A.; Wang, D.; Chen, L.; Sundarraj, R.; Yuchi, Z.; Gong, Y.; Merzendorfer, H. Structural basis for directional chitin biosynthesis. *Nature* **2022**, *610*, 402–408. [CrossRef] [PubMed]
44. Ying, L.; Zining, C.; Jun, H.; Yun, L.; Xinling, Y. Studies on Chitin Synthase Inhibitors. *Prog. Chem.* **2007**, *19*, 535–543.
45. Minfeng, W. Mechanism of Action and Applications of Benzoylurea Insecticides. *For. By-Prod. China* **2023**, *6*, 89–91.

Disclaimer/Publisher's Note: The statements, opinions and data contained in all publications are solely those of the individual author(s) and contributor(s) and not of MDPI and/or the editor(s). MDPI and/or the editor(s) disclaim responsibility for any injury to people or property resulting from any ideas, methods, instructions or products referred to in the content.